The utility of diffusion-weighted T2 mapping for the prediction of histological tumor grade in patients with head and neck squamous cell carcinoma

Noriyuki Fujima[1], Yukie Shimizu[2,3], Masami Yoneyama[4], Junichi Nakagawa[1], Hiroyuki Kameda[2], Taisuke Harada[2], Seijiro Hamada[5], Takayoshi Suzuki[5], Nayuta Tsushima[5], Satoshi Kano[5], Akihiro Homma[5], Kohsuke Kudo[2,3,6]

[1]Department of Diagnostic and Interventional Radiology, Hokkaido University Hospital, Sapporo, Japan; [2]Department of Diagnostic Imaging, Faculty of Medicine and Graduate School of Medicine, Hokkaido University, Sapporo, Japan; [3]Department of Advanced Diagnostic Imaging Development, Faculty of Medicine and Graduate School of Medicine, Hokkaido University, Sapporo, Japan; [4]Philips Japan, Tokyo, Japan; [5]Department of Otolaryngology-Head and Neck Surgery, Faculty of Medicine and Graduate School of Medicine, Hokkaido University, Sapporo, Japan; [6]The Global Station for Quantum Medical Science and Engineering, Global Institution for Collaborative Research and Education, Sapporo, Japan

Contributions: (I) Conception and design: N Fujima, K Kudo; (II) Administrative support: Y Shimizu, J Nakagawa, H Kameda, T Harada; (III) Provision of study materials or patients: S Hamada, T Suzuki, N Tsushima, S Kano, A Homma; (IV) Collection and assembly of data: N Fujima, M Yoneyama; (V) Data analysis and interpretation: N Fujima, M Yoneyama; (VI) Manuscript writing: All authors; (VII) Final approval of manuscript: All authors.

Correspondence to: Noriyuki Fujima, MD, PhD. Department of Diagnostic and Interventional Radiology, Hokkaido University Hospital, N15, W7, Kita-Ku, Sapporo 060-8638, Japan. Email: Noriyuki.Fujima@mb9.seikyou.ne.jp.

Background: In head and neck cancers, histopathological information is important for the determination of the tumor characteristics and for predicting the prognosis. The aim of this study was to assess the utility of diffusion-weighted T2 (DW-T2) mapping for the evaluation of tumor histological grade in patients with head and neck squamous cell carcinoma (SCC).

Methods: The cases of 41 patients with head and neck SCC (21 well/moderately and 17 poorly differentiated SCC) were retrospectively analyzed. All patients received MR scanning using a 3-Tesla MR unit. The conventional T2 value, DW-T2 value, ratio of DW-T2 value to conventional T2 value, and apparent diffusion coefficient (ADC) were calculated using signal information from the DW-T2 mapping sequence with a manually placed region of interest (ROI).

Results: ADC values in the poorly differentiated SCC group were significantly lower than those in the moderately/well differentiated SCC group (P<0.05). The ratio of DW-T2 value to conventional T2 value was also significantly different between poorly and moderately/well differentiated SCC groups (P<0.01). Receiver operating characteristic (ROC) curve analysis of ADC values showed a sensitivity of 0.76, specificity of 0.67, positive predictive value (PPV) of 0.62, negative predictive value (NPV) of 0.8, accuracy of 0.71 and area under the curve (AUC) of 0.73, whereas the ROC curve analysis of the ratio of DW-T2 value to conventional T2 value showed a sensitivity of 0.76, specificity of 0.83, PPV of 0.76, NPV of 0.83, accuracy of 0.8 and AUC of 0.82.

Conclusions: DW-T2 mapping might be useful as supportive information for the determination of tumor histological grade in patients with head and neck SCC.

Keywords: Diffusion; T2 mapping; head and neck squamous cell carcinoma (SCC); histological grade

Introduction

For pretreatment evaluation of patients with head and neck squamous cell carcinoma (SCC), the histological grade as well as the Tumor, Node, Metastasis (TNM) stage classification has been described as an important prognostic factor related to the local control and the prediction of distant metastasis (1,2). Tumor histological grade is usually determined by pathological findings from surgically obtained tumor specimen. However, pathological diagnosis from biopsy-derived tumor tissue is sometimes difficult; a sufficient amount of tumor tissue is not always obtained because of inclusion of peripheral inflammatory tissue, and small biopsy samples don't necessarily reflect the characteristics of the entire tumor (3,4). Other supporting tools are required for the precise histological diagnosis of head and neck SCC.

Quantitative analysis of diffusion-weighted imaging (DWI) is now being investigated for diagnosis, prediction of treatment outcome, and association with tumor genomic information in head and neck SCC (5-8). Notably, the apparent diffusion coefficient (ADC) was previously reported to have a significant correlation with tumor histological grade in head and neck SCC (9,10). Additionally, information on signal intensity obtained from T2-weighted images (T2WI) was also reported to have a relation to tumor histological grade (11). This information can be acquired completely noninvasively, without contrast agent, in MRI. However, each voxel obtained with image analysis includes a mixture of components such as intravascular, extravascular extracellular and intracellular components. Measured signal information in the conventional methodology will suffer from this voxel-wise mixture of signals. In contrast, DWI can depict the signal intensity of each voxel with tissue selectivity depending on its water diffusivity using a diffusion gradient pre-pulse; DWI data with different b-values might help to separate the signals from different components (12-14). In short, effective combination of the signal information obtained from DWI and T2WI-based sequence may reflect the tissue characteristics in greater detail.

In the present study, we developed a new sequence named 'DW-T2 mapping'. This technique combines the characteristics of DWI and T2 mapping by acquiring dual echo signals to calculate the T2 decay under a diffusion-weighted gradient pre-pulse. This sequence enables us to calculate diffusion-restricted-tissue-selective T2 values. The aim of the current study was to evaluate the tissue characteristics of tumor histological grades in head and neck SCC using DW-T2 values. We present the following article in accordance with the STARD reporting checklist (available at https://qims.amegroups.com/article/view/10.21037/qims-22-136/rc).

Methods

Patients

The study was conducted in accordance with the Declaration of Helsinki (as revised in 2013). The protocol of this retrospective study was approved by our institutional review board of Hokkaido University Hospital (No. 021-0025), and individual consent for this retrospective analysis was waived. Patients with head and neck SCC who received pretreatment MRI in our hospital during the period from December 2017 to October 2020 were enrolled consecutively (n=245). This duration was set within the time period during which the specific MR scanning (i.e., DW-T2 mapping) was available in our hospital. From these patients, we selected eligible cases with the following inclusion criteria: (I) the histopathological diagnosis of head and neck SCC was a first-time diagnosis (not a recurrent case); (II) MRI sequences including DW-T2 mapping were performed before any treatment; (III) information regarding histological grade (well, moderately or poorly differentiated SCC) was available in the pathology report. The exclusion criterion was as follows: severe metal or motion artifacts that seriously affected the MR image quality of the primary lesion was present. Finally, total 41 patients were eligible for the current study. All patients were divided into poorly differentiated and well/moderately differentiated SCC groups depending on the description in their pathology reports.

MR imaging protocol

All scanning was performed using a 3.0-Tesla MR unit (Achieva TX; Philips Healthcare, Best, Netherlands) with a 16-channel neurovascular coil. MRI including the DW-T2 map was performed to evaluate the primary tumor lesion.

The sequence design and imaging parameters of the DW-T2 mapping were as follows: spin-echo echo planar imaging (EPI) with fat suppression by spectral adiabatic inversion recovery (SPAIR) pulse, TR 5268 ms, first TE 42.5 ms, second TE 130 ms, slice thickness 5 mm, acquired matrix 112×168, reconstructed matrix by zero filling 256×256, FOV
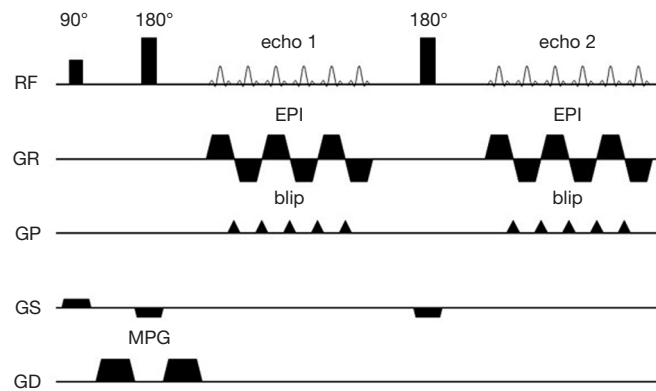
Figure 1 Pulse sequence diagram of dual-echo DWI readout for DW-T2 map. Pulse sequence diagram of DW-T2 map was presented. A bipolar diffusion gradient was inserted as a pre-pulse of T2-map acquisition. To obtain the dual echo of different TEs, this technique uses two 180° refocusing pulses for one 90° excitation pulse. DWI, diffusion weighted imaging; DW-T2, diffusion weighted-T2; EPI, echo planar imaging; RF, radio frequency; GR, gradient pulses for readout; GP, gradient pulses for phase-encoding; GS, gradient pulses for spatial encoding along section; GD, gradient pulses for diffusion-encoding; MPG, motion probing gradient; TE, echo time.

240 mm × 240 mm, inter-slice gap 1.0 mm. The scanning ranges of DW-T2 mapping acquisitions were planned to cover the whole tumor lesion. Two scans with and without a diffusion gradient (b-values of 0 and 1,000 s/mm^2, respectively) were acquired after a 90° excitation pulse and 180° refocusing pulse. The pulse sequence chart is presented in *Figure 1*. Finally, four types of image datasets, with short or long TE (42.5 and 130 ms) with and without a diffusion gradient (b=0, 1,000) were obtained.

Axial T1 weighted images (T1WI) and fat-suppressed T2WI (Fs-T2WI) were also acquired with following parameter settings: (I) T1WI; a spin-echo sequence, TR 450 ms, TE 10 ms, FOV, 240 mm × 240 mm, 512×512 matrix, slice thickness 5 mm, (II) Fs=T2WI, a turbo spin-echo sequence, TR 4,500 ms, TE 70 ms, TSE factor 9, FOV, 240 mm × 240 mm, 512×512 matrix, slice thickness 5 mm.

Data analysis: parameter map creation and ROI delineation

From the four image datasets obtained by DW-T2 mapping sequence, short TE without a diffusion gradient (TE 42.5 ms, b=0), short TE with a diffusion gradient (TE 42.5 ms, b=1,000), long TE without a diffusion gradient (TE 130 ms, b=0) and long TE with a diffusion gradient (TE 130 ms, b=1,000), we created a conventional T2 map, an ADC map and a DW-T2 map. The conventional T2 map was obtained by calculating the signal decay between short and

long TE images without a diffusion gradient. The DW-T2 map was obtained by calculating the signal decay between short and long TE with a diffusion gradient (b=1,000). The signal intensity arising from water-diffusion-restricted space (e.g., cellular space or narrowed extravascular extracellular space) will be the only remaining signal under acquisition with high b-value diffusion gradient (b=1,000); therefore, DW-T2 mapping was thought to calculate the T2 value of pathologically specific areas in the cancer tissue of such diffusion-restricted space. Finally, an ADC map was obtained by calculating the signal intensity difference between short TE images with and without a diffusion gradient. The calculation process was performed by using the self-developed program by MATLAB ver. 2019a (MathWorks, Natick, MA). A representative case of parameter calculation is presented in *Figure 2*.

A board-certified neuroradiologist with 13 years of experience in head and neck radiology who was blinded to the pathological information delineated each tumor with a polygonal region of interest (ROI) on short TE (42.5 ms) without diffusion gradient (b=0) images in the DW-T2 mapping sequence. The axial T1WI and Fs-T2WI as well as other image datasets in DW-T2 mapping were used as references for ROI delineation. Any area suspected of being necrotic or cystic was excluded from the ROI; only solid components of the tumor was included in the ROI. If the tumor extended into two or more slices, the slice in which the largest area of tumor was depicted was selected. Thereafter, the tumor ROI was copied onto the conventional
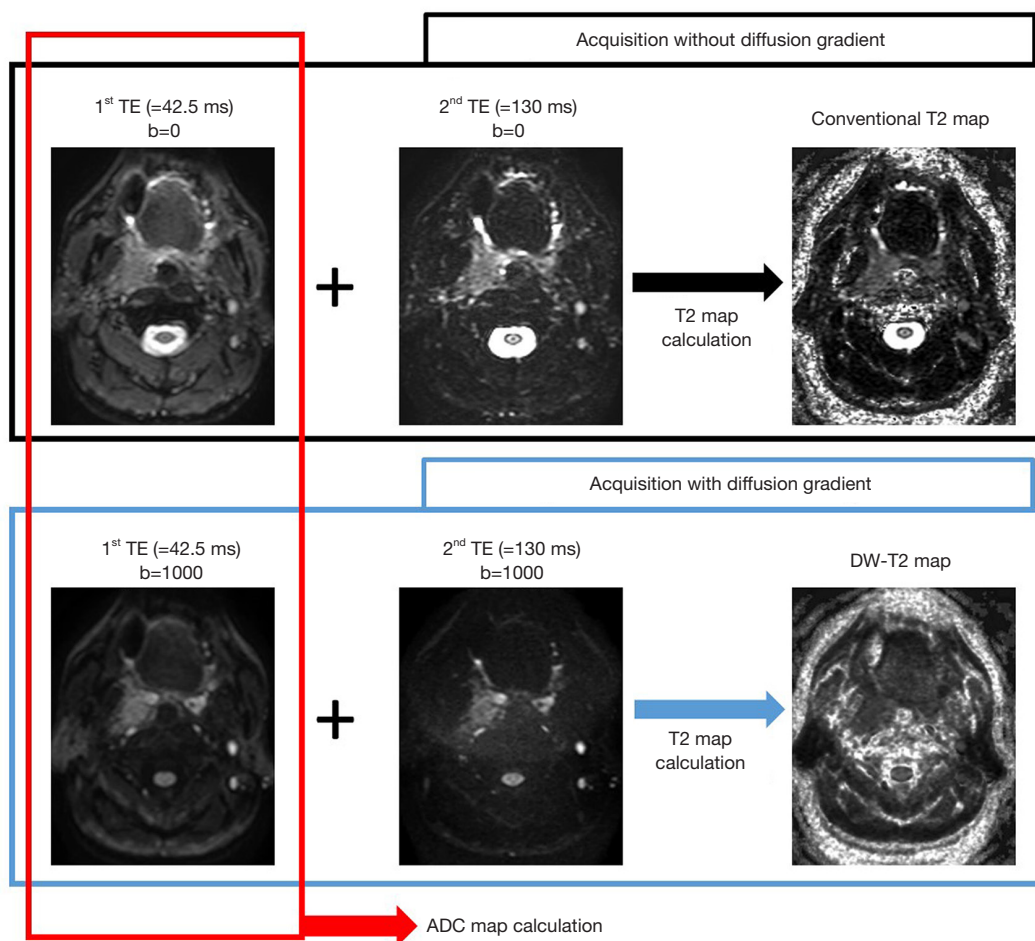
Figure 2 Diagram of parameter calculation. From the DW-T2 mapping sequence, four types of images were obtained: (I) short TE (42.5 ms) without a diffusion gradient (b=0), (II) short TE (42.5 ms) with a diffusion gradient (b=1,000), (III) long TE (130 ms) without a diffusion gradient (b=0); (IV) long TE (130 ms) with a diffusion gradient (b=1,000). Conventional T2 values were calculated using image data from short TE and long TE (42.5 and 130 ms) without a diffusion gradient (b=0), whereas DW-T2 values were calculated using image data from short TE and long TE (42.5 and 130 ms) with a diffusion gradient (b=1,000). In addition, ADC values were calculated using short TE (42.5 ms) with and without a diffusion gradient (b=0 and 1,000). TE, echo time; DW-T2, diffusion weighted-T2; ADC, apparent diffusion coefficient.

T2 map, DW-T2 map and ADC map. The voxel-wise T2 values, DW-T2 values and ADC values in each tumor were calculated as mean values for the ROI. The ratio of DW-T2 value to conventional T2 value was also obtained by dividing the DW-T2 by the conventional T2 value.

Statistical analysis

The conventional T2 value, DW-T2 value, ADC value and the ratio of DW-T2 value to conventional T2 value were respectively compared between patient groups with poorly differentiated and moderately/well differentiated SCCs by Mann Whitney U test. If a significant difference between poorly and moderately/well differentiated SCC groups was observed in one or more parameters, such parameters were further assessed using receiver operating characteristic (ROC) curves constructed for calculating the area under the curve (AUC). The sensitivity, specificity, positive predictive value (PPV), negative predictive value (NPV) and diagnostic accuracy were calculated with the optimal cut-off value determined by the Youden Index in ROC curve analysis. P values <0.05 were considered significant. SPSS software (IBM, Armonk, NY) was used for all statistical analyses.

4028

Fujima et al. DW-T2 mapping for head and neck SCC
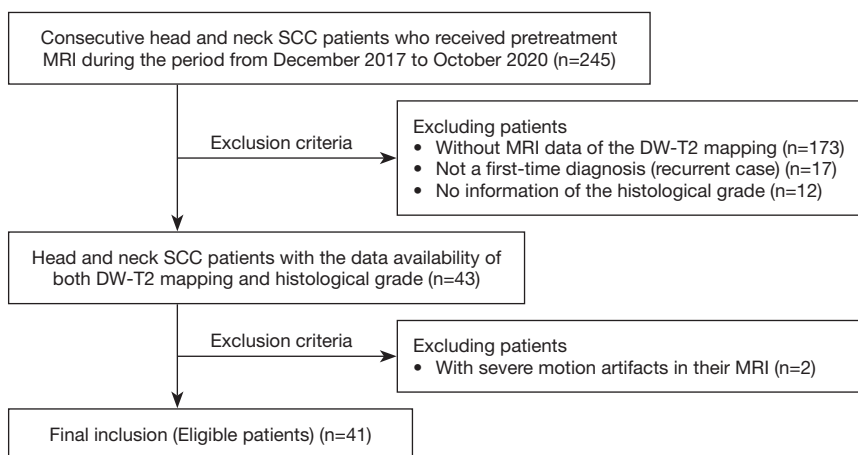
Figure 3 Flow diagram of the study population. DW-T2, diffusion weighted-T2; MRI, magnetic resonance imaging; SCC, squamous cell carcinoma.

Results

In total of 245 consecutive patients, the cases of 43 patients were selected with the inclusion criteria, thereafter, two patients were excluded with the exclusion criteria; total 41 patients were finally selected as the study population. The process of patient selection was presented in *Figure 3*. Of all 41 patients, 17 patients were classified as poorly differentiated SCC whereas 24 patients were classified as moderately/well differentiated SCC. Detailed patient characteristics of both groups are provided in *Table 1*.

Comparisons of each parameter in poorly and moderately/well differentiated SCC groups are presented in *Table 2*. The ADC value was significantly lower in the poorly differentiated SCC group than the moderately/well differentiated SCC group ($P<0.05$). The ratio of the DW-T2 value to the conventional T2 value was also significantly lower in the poorly differentiated SCC group than the moderately/well differentiated SCC group ($P<0.01$).

The ROC curve analysis of the ADC value showed an AUC of 0.73 (95% confidence intervals: 0.56–0.88), with the sensitivity of 0.76, specificity of 0.67, PPV of 0.62, NPV of 0.8 and the accuracy of 0.71, whereas the ROC curve analysis of the ratio of DW-T2 value to conventional T2 value showed an AUC of 0.82 (95% confidence intervals: 0.69–0.96), with sensitivity of 0.76, specificity of 0.83, PPV of 0.76, NPV of 0.83 and the accuracy of 0.8. ROC curves are shown in *Figure 4*.

Discussion

Our results suggested that significant differences in the

ADC and ratio of DW-T2 value to conventional T2 value were observed between the poorly differentiated SCC and moderately/well differentiated SCC patient groups. The ratio of DW-T2 value to conventional T2 value was determined to have the most powerful diagnostic performance.

Tumor histological grade is an important determinant in the prognosis of head and neck SCC. Specifically, tumor histologic differentiation was reported to relate to nodal disease, distant metastasis, locoregional recurrence and the patient survival rate (1,2). Therefore, pre-treatment assessment of histological differentiation can be clinically important for patients with head and neck SCC. A surgical procedure is usually performed to obtain tumor tissue for the diagnosis of tumor differentiation by histopathological assessment, which is considered the gold standard for the diagnosis of tumor histological grade. However, surgical biopsy samples often contain peripheral inflammatory tissue that muddies the diagnosis; moreover, a small tissue biopsy sample is often insufficient to characterize the entire tumor, especially in cases of intratumoral heterogeneity (3,4). Our results suggest that DW-T2 mapping might have potential for use as a supportive tool for the diagnosis of tumor histological grade in patients with head and neck SCC and will provide clinically useful information.

The T2 relaxation time reflects numerous tissue characteristics (15). A previous investigation reported the difference of signal intensity in Fs-T2WI between poorly and moderately/well differentiated head and neck SCCs (11). In that study, the signal intensity difference in Fs-T2WI

Table 1 Patient characteristics

Characteristics	Total	Moderately/well differentiated SCC	Poorly differentiated SCC
Number	41	24	17
Age, years			
Range	41–85	41–85	47–85
Median	66	64	67
Gender			
Male	32	18	14
Female	9	6	3
Subsite			
Oropharynx (HPV positive)	9	5	4
Oropharynx (HPV negative)	13	7	6
Hypopharynx	9	6	3
Oral cavity	7	4	3
Sinonasal cavity	3	2	1
T-stage			
T1	0	0	0
T2	20	11	9
T3	15	9	6
T4a,b	6	4	2
N-stage			
N0	13	9	4
N1	11	7	4
N2a-c	12	5	7
N3a,b	5	3	2

SCC, squamous cell carcinoma; HPV, human papillomavirus.

was attributed to possible differences in several histological intratumoral characteristics such as tumor cell density, extravascular extracellular space, and micronecrosis. Despite the statistical significance of their findings, a certain degree of overlap in the T2WI signal intensities of poorly and moderately/well differentiated SCCs remained. Various histopathological components like tumor cells, extravascular extracellular space and the micronecroses might have different T2 values, respectively, and the visible signal intensity in each pixel on T2WI will be present as a rough average of the T2 values of these components; this produces uncertainties in interpreting the tumor signal information in T2WI. By contrast, the present study revealed that the ratio of the DW-T2 value to the conventional T2 value was significantly different between moderately/well and poorly differentiated SCCs. Specifically, most cases of moderately/ well differentiated SCC displayed a lower T2 value in the acquisition of DW-T2 compared to conventional T2, whereas most cases of poorly differentiated SCCs showed no marked difference in T2 value between the acquisitions of the conventional T2 and DW-T2 mapping (a larger ratio value). The degree of decrease of DW-T2 from the conventional T2 value possibly reflects the structural features of different components (i.e., tumor cell density, the amount of stromal tissue, the presence of micronecrosis) to some extent. Semi-quantitative evaluation using DW-T2 mapping might successfully detect such feature differences among SCCs with different histological grades.

As another result of the current study, the ADC value was lower in poorly differentiated SCCs than in moderately/ well differentiated SCCs. Consistent with our result, several past reports have also noted that ADC values obtained from DWI datasets were useful for the determination of tumor histological grades (9,10). In one of these reports, the lower ADC was attributed to the higher cellular density and limited extracellular extravascular space observed in

Table 2 Differences in parameters according to histological grade

	Moderately/well differentiated SCC	Poorly differentiated SCC	P value
Conventional T2 value	76.8±11.2	69.1±11.6	0.07
DW-T2 value	69.1±7.4	68.4±10.6	0.42
Ratio of DW-T2 value to conventional T2 value	0.89±0.09	0.99±0.06	0.002*
ADC value	0.98±0.16	0.87±0.11	0.03*

Data are mean ± standard deviation. *, statistical significance. DW-T2, diffusion weighted T2; ADC, apparent diffusion coefficient; SCC, squamous cell carcinoma.
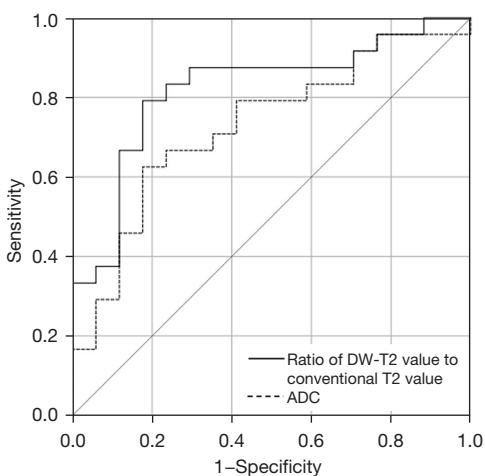
Figure 4 ROC curve analysis for the discrimination of histological grades. ROC curves for the discrimination of poorly and moderately/well differentiated SCC by the ratio of conventional T2 value to DW-T2 value and the ADC value are respectively presented. The ratio of the conventional T2 value to the DW-T2 value had an AUC of 0.82 and the ADC value had an AUC of 0.73. DW-T2, diffusion weighted-T2; ADC, apparent diffusion coefficient; ROC, receiver operating characteristic; SCC, squamous cell carcinoma; AUC, area under the curve.

poorly differentiated SCCs. Another report speculated that the loss of both keratinization and intercellular bridges in poorly differentiated SCC causes the overall compaction of intratumoral tissue, resulting in a lower ADC value. While ADC can be considered a useful tool to support distinction of histological grades, the diagnostic performance obtained from the dataset of DW-T2 mapping was suggested to be superior to that of ADC values in the current study. We speculate that it is the combined use of both diffusion-related information and tissue T2 values acquired from DW-T2 mapping that allows higher diagnostic performance for distinguishing between poorly differentiated SCCs and moderately/well differentiated SCCs. For instance, narrow extracellular extravascular space might be somewhat difficult to be distinguish from cellular space because both components are characterized as areas with restricted diffusion; the added information of T2 value could successfully distinguish these two types of tissue as having different T2 value ranges. In a clinical setting, DW-T2 mapping with its quantitative assessment can be helpful as an additional supporting tool in predicting the histological diagnosis.

The prediction of tumor histological grade in head and neck SCCs will contribute to the decision-making process regarding the details of the treatment strategy (e.g., surgical treatment, type of chemotherapy and radiotherapy). Specifically, poorly differentiated SCCs have a relatively high sensitivity to chemoradiotherapy; supportive assessment related to this histological information might be demonstrated quantitatively by using the DW-T2 mapping technique.

The current study has several limitations. First, the number of patients was small. The limited case numbers in the two groups of well/moderately and poorly differentiated SCCs limits statistical power. However, we believe that the significant difference in the ratio of the DW-T2 value to the conventional T2 value between the two groups is reliable to a degree, because the level of statistical significance was high (P=0.002), even for an analysis with such a small number of patients. In contrast, diagnostic performance values (e.g., AUC, accuracy) may be slightly different if we re-analyze diagnostic performance with a large number of patients; further analysis with a large number of patients will be needed to address this limitation. Second, several different primary sites, such as the oropharyngeal, hypopharyngeal, oral and sinonasal cavities, were represented in the patient cohort. In addition, we investigated tumors in primary sites only, however, there might be a certain degree of difference in the quantitative values between the primary and nodal sites even in the same patient. Further subgroup analysis dividing primary sites by location and comparing between primary and nodal sites should be performed to clarify these issues. Third, we only assessed tumor histological grade; other clinically important factors such as human papillomavirus (HPV) status (16), the specific genomic status (17) and other important histopathological characteristics such as the presence of lymphovascular invasion or perineural invasion (18) were not considered. For the purposes of the present study, a preliminary investigation with a small number of patients, we included oropharyngeal SCC patients with both HPV-positive and -negative statuses. The usual histological grading may not be applicable in the case of HPV-associated SCCs; therefore, additional analysis excluding HPV-positive oropharyngeal SCCs will be needed, using a sufficient number of oropharyngeal SCC patients.

Conclusions

The technique of DW-T2 mapping has the possibility to

provide supportive information for the determination of tumor histological grade in patients with head and neck SCC by the effective combination of T2 values and tumor diffusion information. This technique might contribute to the pretreatment assessment of patients with head and neck SCC.

Acknowledgments

Footnote

Reporting Checklist: The authors have completed the STARD reporting checklist. Available at https://qims.amegroups.com/article/view/10.21037/qims-22-136/rc

Conflicts of Interest: All authors have completed the ICMJE uniform disclosure form (available at https://qims.amegroups.com/article/view/10.21037/qims-22-136/coif). NF reports that this work was supported by the Japan Society for the Promotion of Science (JSPS) KAKENHI (No. JP21K07558). MY reports that MY is currently employed by Philips Japan. The other authors have no conflicts of interest to declare.

Ethical Statement: The authors are accountable for all aspects of the work in ensuring that questions related to the accuracy or integrity of any part of the work are appropriately investigated and resolved. The study was conducted in accordance with the Declaration of Helsinki (as revised in 2013). The study was approved by institutional review board of Hokkaido University Hospital (No. 021-0025) and individual consent for this retrospective analysis was waived.

Open Access Statement: This is an Open Access article distributed in accordance with the Creative Commons Attribution-NonCommercial-NoDerivs 4.0 International License (CC BY-NC-ND 4.0), which permits the non-commercial replication and distribution of the article with the strict proviso that no changes or edits are made and the original work is properly cited (including links to both the formal publication through the relevant DOI and the license). See: https://creativecommons.org/licenses/by-nc-nd/4.0/.

References

1. Janot F, Klijanienko J, Russo A, Mamet JP, de Braud F, El-Naggar AK, Pignon JP, Luboinski B, Cvitkovic E. Prognostic value of clinicopathological parameters in head and neck squamous cell carcinoma: a prospective analysis. Br J Cancer 1996;73:531-8.
2. Coca-Pelaz A, Rodrigo JP, Suárez C. Clinicopathologic analysis and predictive factors for distant metastases in patients with head and neck squamous cell carcinomas. Head Neck 2012;34:771-5.
3. Götte K, Schäfer C, Riedel F, Arens N, Hörmann K. Intratumoral genomic heterogeneity in primary head and neck cancer and corresponding metastases detected by dual-FISH. Oncol Rep 2004;11:17-23.
4. Jacob R, Welkoborsky HJ, Mann WJ, Höfken F, Dienes HP, Freije JE. Heterogeneity of squamous cell carcinomas of the head and neck--analysis of tumor biologic factors and proliferation rates. Laryngoscope 1996;106:1170-5.
5. Bhatnagar P, Subesinghe M, Patel C, Prestwich R, Scarsbrook AF. Functional imaging for radiation treatment planning, response assessment, and adaptive therapy in head and neck cancer. Radiographics 2013;33:1909-29.
6. King AD, Thoeny HC. Functional MRI for the prediction of treatment response in head and neck squamous cell carcinoma: potential and limitations. Cancer Imaging 2016;16:23.
7. Payabvash S. Quantitative diffusion magnetic resonance imaging in head and neck tumors. Quant Imaging Med Surg 2018;8:1052-65.
8. Srinivasan A, Mohan S, Mukherji SK. Biologic imaging of head and neck cancer: the present and the future. AJNR Am J Neuroradiol 2012;33:586-94.
9. Ahn SJ, Choi SH, Kim YJ, Kim KG, Sohn CH, Han MH, Chang KH, Min HS. Histogram analysis of apparent diffusion coefficient map of standard and high B-value diffusion MR imaging in head and neck squamous cell carcinoma: a correlation study with histological grade. Acad Radiol 2012;19:1233-40.
10. Yun TJ, Kim JH, Kim KH, Sohn CH, Park SW. Head and neck squamous cell carcinoma: differentiation of histologic grade with standard- and high-b-value diffusion-weighted MRI. Head Neck 2013;35:626-31.
11. Fujima N, Homma A, Harada T, Shimizu Y, Tha KK, Kano S, Mizumachi T, Li R, Kudo K, Shirato H. The utility of MRI histogram and texture analysis for the prediction of histological diagnosis in head and neck malignancies. Cancer Imaging 2019;19:5.

12. Le Bihan D, Breton E, Lallemand D, Grenier P, Cabanis E, Laval-Jeantet M. MR imaging of intravoxel incoherent motions: application to diffusion and perfusion in neurologic disorders. Radiology 1986;161:401-7.

13. Panagiotaki E, Walker-Samuel S, Siow B, Johnson SP, Rajkumar V, Pedley RB, Lythgoe MF, Alexander DC. Noninvasive quantification of solid tumor microstructure using VERDICT MRI. Cancer Res 2014;74:1902-12.

14. Fujima N, Yoshida D, Sakashita T, Homma A, Tsukahara A, Tha KK, Kudo K, Shirato H. Intravoxel incoherent motion diffusion-weighted imaging in head and neck squamous cell carcinoma: assessment of perfusion-related parameters compared to dynamic contrast-enhanced MRI. Magn Reson Imaging 2014;32:1206-13.

15. Herfkens R, Davis P, Crooks L, Kaufman L, Price D, Miller T, Margulis AR, Watts J, Hoenninger J, Arakawa M, McRee R. Nuclear magnetic resonance imaging of the abnormal live rat and correlations with tissue characteristics. Radiology 1981;141:211-8.

16. Ang KK, Harris J, Wheeler R, Weber R, Rosenthal DI, Nguyen-Tân PF, Westra WH, Chung CH, Jordan RC, Lu C, Kim H, Axelrod R, Silverman CC, Redmond KP, Gillison ML. Human papillomavirus and survival of patients with oropharyngeal cancer. N Engl J Med 2010;363:24-35.

17. Ock CY, Son B, Keam B, Lee SY, Moon J, Kwak H, Kim S, Kim TM, Jeon YK, Kwon SK, Hah JH, Lee SH, Kwon TK, Kim DW, Wu HG, Sung MW, Heo DS. Identification of genomic mutations associated with clinical outcomes of induction chemotherapy in patients with head and neck squamous cell carcinoma. J Cancer Res Clin Oncol 2016;142:873-83.

18. Shen H, Huang Y, Yuan X, Liu D, Tu C, Wang Y, Li X, Wang X, Chen Q, Zhang J. Using quantitative parameters derived from pretreatment dual-energy computed tomography to predict histopathologic features in head and neck squamous cell carcinoma. Quant Imaging Med Surg 2022;12:1243-56.